Molecular Therapy
Oncolytics
Original Article

Newly Characterized Murine Undifferentiated Sarcoma Models Sensitive to Virotherapy with Oncolytic HSV-1 M002

Eric K. Ring,[1] Rong Li,[2] Blake P. Moore,[1] Li Nan,[1] Virginia M. Kelly,[1] Xiaosi Han,[3] Elizabeth A. Beierle,[4] James M. Markert,[5] Jianmei W. Leavenworth,[5] G. Yancey Gillespie,[5] and Gregory K. Friedman[1]

[1]Division of Pediatric Hematology and Oncology, Department of Pediatrics, University of Alabama at Birmingham, Birmingham, AL 35233, USA; [2]Neuropathology, Children's of Alabama, Birmingham, AL 35233, USA; [3]Department of Neurology, University of Alabama at Birmingham, Birmingham, AL 35233, USA; [4]Department of Surgery, University of Alabama at Birmingham, Birmingham, AL 35233, USA; [5]Department of Neurosurgery, University of Alabama at Birmingham, Birmingham, AL, USA 35233

Despite advances in conventional chemotherapy, surgical techniques, and radiation, outcomes for patients with relapsed, refractory, or metastatic soft tissue sarcomas are dismal. Survivors often suffer from lasting morbidity from current treatments. New targeted therapies with less toxicity, such as those that harness the immune system, and immunocompetent murine sarcoma models to test these therapies are greatly needed. We characterized two new serendipitous murine models of undifferentiated sarcoma (SARC-28 and SARC-45) and tested their sensitivity to virotherapy with oncolytic herpes simplex virus 1 (HSV-1). Both models expressed high levels of the primary HSV entry molecule nectin-1 (CD111) and were susceptible to killing by interleukin-12 (IL-12) producing HSV-1 M002 in vitro and in vivo. M002 resulted in a significant intratumoral increase in effector CD4$^+$ and CD8$^+$ T cells and activated monocytes, and a decrease in myeloid-derived suppressor cells (MDSCs) in immunocompetent mice. Compared to parent virus R3659 (no IL-12 production), M002 resulted in higher CD8:MDSC and CD8:T regulatory cell (Treg) ratios, suggesting that M002 creates a more favorable immune tumor microenvironment. These data provide support for clinical trials targeting sarcomas with oncolytic HSV-1. These models provide an exciting opportunity to explore combination therapies for soft tissue sarcomas that rely on an intact immune system to reach full therapeutic potential.

INTRODUCTION

Sarcomas are a heterogeneous group of rare malignant tumors involving bone and soft tissue. They represent approximately 1%–2% and 6%–15% of adult and pediatric tumors, respectively.[1–3] The mainstay of therapy includes various combinations of surgery, cytotoxic chemotherapy, and radiation, which have therapeutic limits because of life-threatening toxicities. Furthermore, in children these treatments impair normal development and result in long-term morbidities. Adult survivors of childhood sarcoma have an almost 10-fold risk of developing a second primary neoplasm and are more likely to have limited physical function and chronic pain compared to the general population.[4] Although current therapies have improved survival rates for adults and children with sarcomas, outcomes remain extremely poor for patients with relapsed, refractory, or metastatic disease. At diagnosis, survival can be as high as 90% for patients with localized disease with favorable features, but plummets to <20% for patients with metastatic disease.[5,6] Relapsed disease can be especially ominous as survival rates fall to <15%.[7–9]

Herpes simplex virus 1 (HSV-1) has been successfully engineered for oncolytic HSV (oHSV) therapy by introducing mutations in both copies of the $\gamma_1$34.5 gene in order to prevent a productive infection in normal cells while maintaining the virus's oncolytic activity against cancer cells.[10] In addition to killing cancer cells directly, the virus is immunogenic; as the virus lyses tumor cells and creates inflammation, newly exposed cancer antigens may be cross-presented, triggering both an innate and an adaptive anti-tumor immune response. The HSV-1 genome is ∼154 Kb, but ∼30 Kb contain genes nonessential for viral replication in tumor cells and can be removed to accommodate insertion of therapeutic genes. oHSV M002 produces a physiologically relevant amount of murine interleukin-12 (IL-12), a cytokine with potent antitumor properties that has been inserted into both loci occupied by $\gamma_1$34.5.[11] IL-12 is normally produced by antigen-presenting cells (APCs), including B lymphocytes, dendritic cells, and mononuclear phagocytes. It enhances the cytolytic activity of natural killer (NK) cells and cytotoxic T cells, and promotes the development of a T helper 1 (Th1)-type immune response.[12,13] In mice bearing intracranial gliomas, treatment with M002 significantly improved survival compared to treatment with the parent HSV R3659, which lacks IL-12.[14] M032, which produces human IL-12, was safe in nonhuman

Received 3 May 2017; accepted 6 September 2017;
https://doi.org/10.1016/j.omto.2017.09.003.

Correspondence: Gregory K. Friedman, Division of Pediatric Hematology and Oncology, Department of Pediatrics, University of Alabama at Birmingham, 1600 7th Avenue South, Lowder 512, Birmingham, AL 35233, USA.
E-mail: gfriedman@peds.uab.edu

This is an open access article under the CC BY-NC-ND license (http://creativecommons.org/licenses/by-nc-nd/4.0/).

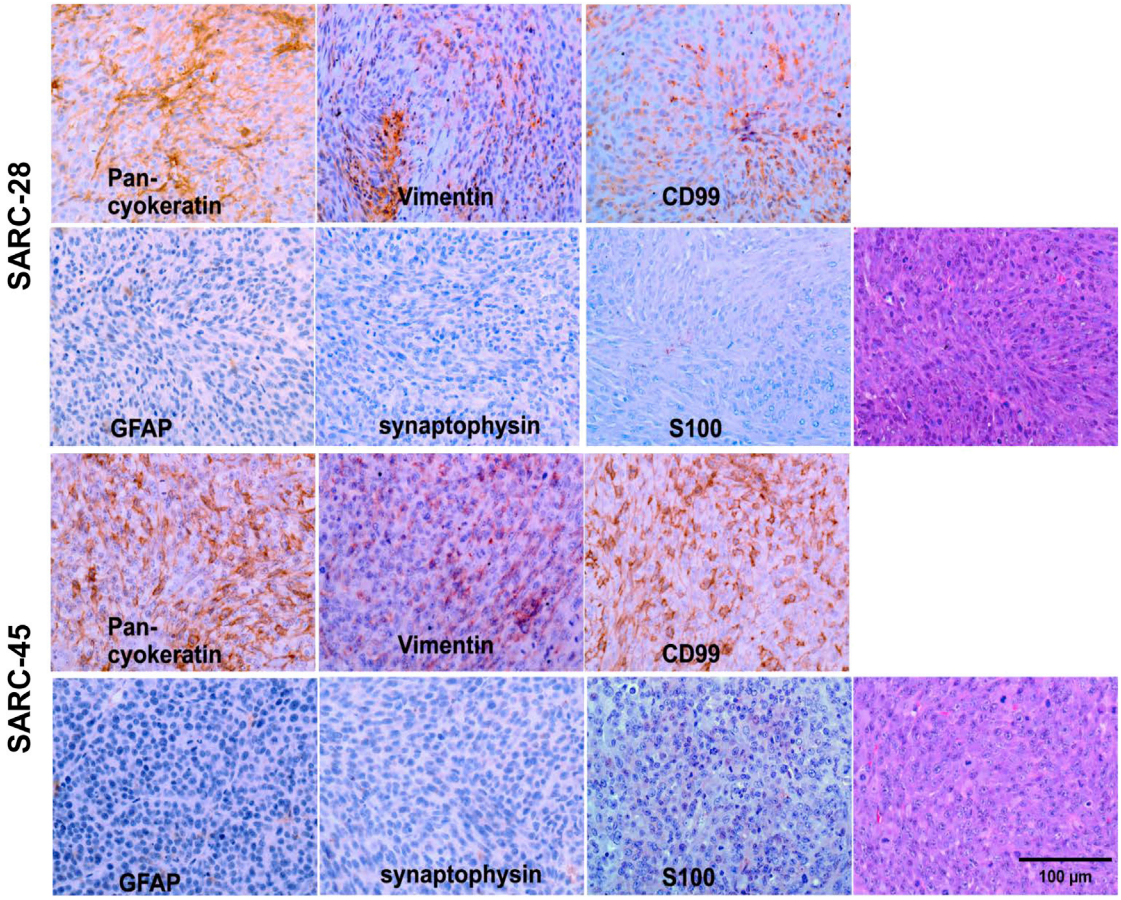

Figure 1. Immunohistochemical Profiles and Morphological Features of SARC-28 and SARC-45
Both tumors were consistent with murine undifferentiated sarcoma. Photomicrographs are representative of 10 sections.

primates leading to a current phase I clinical trial in adults with recurrent malignant glioma (NCT02062827).[15]

Rapidly emerging therapies such as oncolytic virotherapy, tumor vaccines, and immune checkpoint blockade all rely on an intact host immune system to be effective. These are attractive approaches for patients with bone and soft tissue sarcomas; however, a major challenge for developing and testing immunotherapies against these tumors is the lack of available immunocompetent murine models that allow examination of treatment response with an intact immune system. We sought to characterize two new serendipitous models of murine undifferentiated soft tissue sarcoma, SARC-28 and SARC-45, and to determine their susceptibility to oHSV and their suitability as models for testing other immunotherapeutics.

RESULTS

Immunohistochemistry of Murine Sarcomas

SARC-28 and SARC-45 are murine sarcomas that apparently arose spontaneously in immunocompromised C.B-17 severe combined immunodeficiency (SCID) mice during serial transplantation of patient-derived xenografts established by direct implantation of freshly resected human medulloblastoma tissues, BT-28 and BT-45.[16] Short tandem repeat analyses performed by the University of Alabama at Birmingham (UAB) Heflin Center for Genomic Science repeatedly on the tumors revealed the absence of human DNA. At that point, tumors were harvested and stained for further evaluation. Both tumor lines (SARC-28 and SARC-45) demonstrated similar findings, and based on histopathology and immunohistochemical features, the tumors were most consistent with high-grade undifferentiated murine sarcoma (Figure 1) and were inconsistent with pediatric human medulloblastoma, which was the tumor type originally implanted in mice. Microscopic examination demonstrated a well-circumscribed unencapsulated hypercellular malignant tumor composed of relatively uniform plump spindle cells with high nuclear/cytoplasm ratio, tapering nuclei, and indistinct cell border. Mitotic activity was brisk. The tumor cells were arranged in short fascicles or solid sheets. Foci of necrosis (SARC-45) were present. Immunohistochemically, the tumor cells showed patchy immunoreactivity for CD99, vimentin (weak), and cytokeratin (Figure 1, upper panels). Immunostains

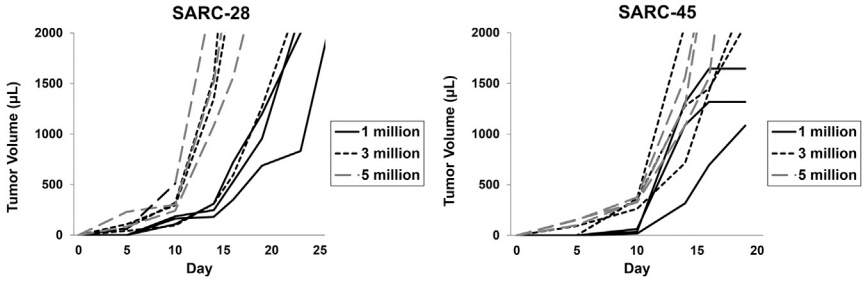

Figure 2. Representative Tumor Growth of SARC-28 and SARC-45

Tumors were grown in BALB/c mice after flank injection of 1, 3, or 5 million cells, and tumor volume was measured.

for glial fibrillary acidic protein (GFAP), synaptophysin, and S100 were negative (Figure 1, lower panels).

In Vivo Tumor Growth and Doubling Time

Mice were injected with 1, 3, or 5 million cells in the flank, tumor size was measured, and doubling time was calculated (Figure 2). Doubling time in vivo for 1 million cells of SARC-28 or SARC-45 was 2.02 ± 0.55 and 1.69 ± 0.65 days, respectively.

Expression of HSV Entry Molecules

Freshly disaggregated cells from SARC-28 and SARC-45 were assessed for expression of nectin-1 (CD111), a cell surface adhesion molecule found in a variety of tissues that is the most efficient entry receptor for HSV, as well as other reported HSV entry molecules: nectin-2 (CD112), herpes virus entry mediator (HVEM; CD270), and heparan sulfate proteoglycan (syndecan-2).[17] Both sarcomas showed high expression of the primary HSV entry molecule CD111 and high expression of other entry molecules including CD112, CD270, and syndecan-2, suggesting that HSV should readily be able to enter the tumor cells (Table 1).

In Vitro Cytotoxicity

We next tested cells from both sarcomas for sensitivity to oHSV M002 by adding graded doses of virus. Both tumors were highly sensitive to killing by M002 (Figure 3A). The lethal dose of virus required to kill 50% of SARC-28 and SARC-45 cells was 2.9 ± 0.1 and 0.4 ± 0.02 plaque-forming units (PFU)/cell, respectively.

Viral Replication

To assess for M002 virus replication in SARC-28 and SARC-45, we infected monolayers of cells with 0.1 PFU/cell and at 24 hr post-infection, viral titers were determined. Mock infection with vehicle appropriately showed no plaque formation. M002 replicated to a titer of $5.7 \pm 2.3 \times 10^5$ PFU/mL in SARC-28 and $5.7 \pm 2.5 \times 10^5$ PFU/mL in SARC-45, suggesting M002 readily infects and efficiently replicates in both tumor models (Figure 3B).

In Vivo Oncolytic Effect of M002

To measure the oncolytic effect of M002 in vivo, we used an immunodeficient athymic nude model in an immunoprivileged site (brain). Mice were injected with 2×10^5 SARC-28 or 5×10^5 SARC-45 cells into the right caudate nucleus. Three days later, mice received a single 1×10^7 PFU dose of M002 or saline into the site where the tumor cells were injected. This time point and cell number were chosen because of the fast-growing nature of the tumor. Mean survival time (MST) was significantly prolonged (79 ± 31.8 versus 11 ± 0 days; $p = 0.003$) in SARC-28 with six long-term survivors at 120 days compared to zero survivors in the saline-treated group (Figure 4). Similarly, MST was extended in mice bearing intracranial SARC-45 tumors after treatment with M002 (46.7 ± 16.4 versus 11.2 ± 0.5 days; $p = 0.002$) with three long-term survivors at 120 days compared to zero survivors in the saline-treated group (Figure 4). This suggests that the oncolytic effect of the virus in the face of minimal disease is robust in these tumor models.

In Vivo Cytotoxicity in Immunocompetent Model

To determine whether a single dose of M002 could prolong survival in immunocompetent mice and to determine immune effects of M002, we injected mice bearing SARC-28 or SARC-45 intratumorally with either saline, M002, or R3659, the parent virus of M002 without the murine IL-12 gene. Tumor growth was inhibited (Figure 5A), and MST was significantly prolonged in mice bearing SARC-28 after treatment with a single 1×10^7 PFU dose of R3659 (20.9 ± 0.8 days) or M002 (20.2 ± 0.8 days) compared to saline alone (16.4 ± 0.6 days) (Figure 5C). Similarly, in mice bearing SARC-45, tumor growth was inhibited (Figure 5B) and MST was significantly prolonged after treatment with a single 1×10^7 PFU dose of M002 (25.7 ± 4.9 days) or R3659 (23.3 ± 3.9 days) compared to saline alone (18.3 ± 1.9 days) (Figure 5D). In both models, there was not a significant survival advantage in mice treated with M002 compared to R3659.

Immune Response Study

To assess the immune response to treatment with M002, we harvested SARC-28 tumors from immunocompetent mice 0, 3, and 10 days after a single intratumoral injection with saline, R3659, or M002 and analyzed them by flow cytometry (Figure 6A). Compared to treatment with saline alone, tumors treated with M002 demonstrated a 9-fold and 6-fold increase in the proportion of $CD4^+$ ($CD45^+CD4^+CD3^+$) and $CD8^+$ ($CD45^+CD8^+CD3^+$) cells, respectively, on day 3, and a 5-fold and 2-fold increase in $CD4^+$ and $CD8^+$ cells on day 10 (Figure 6B). In addition to the increased percentage of $CD4^+$ and $CD8^+$ cells, treatment with M002 resulted in a pronounced increase in the proportion of effector immune cells including effector $CD4^+$ ($CD45^+CD4^+CD3^+IFN^+$), effector $CD8^+$ ($CD45^+CD8^+CD3^+IFN^+$granzyme B^+), and activated monocytes ($CD45^+CD11b^+Gr1^{HI}$) (Figure 6C). Of note, tumors treated with M002 demonstrated an 8-fold and 3-fold increase in activated monocytes on days 3 and 10, respectively, compared to tumors treated with saline. While M002 resulted in a significant decrease in intratumoral myeloid-derived suppressor cells (MDSCs; $CD45^+CD11b^+Gr1^{+INT}$) compared to saline,

Table 1. Percent of Cells Expressing HSV Entry Molecules

Cell Line	CD111	CD112	CD270	SDC2
SARC-28	83.8 ± 1.6	80.9 ± 1.6	64.9 ± 3.2	71.5 ± 9.1
SARC-45	91.7 ± 7.2	96.4 ± 1.1	69.4 ± 6.7	92.4 ± 0.6

Values are mean ± SD.

the proportion of T regulatory cells (Tregs; $CD45^+CD4^+CD3^+CD25^+$ $FoxP3^+$) was increased (Figure 6D). Compared to R3659, treatment with M002 resulted in an increased percentage of $CD8^+$ cells and activated monocytes and a decreased percentage of MDSCs (Figures 6B–6D). Furthermore, the CD8:MDSC and CD8:Treg ratios were 4.9-fold and 1.6-fold higher at day 10 in M002 compared to R3659, suggesting that M002 creates a more favorable immune tumor microenvironment.

DISCUSSION

Despite advances in conventional chemotherapy, surgical techniques, and radiation therapy, outcomes for patients with relapsed, refractory, or metastatic sarcomas are dismal.[5,6] The rarity of bone and soft tissue sarcomas, and the paucity of reliable preclinical sarcoma models make studying novel therapies to target this disease difficult. With the emergence of therapies that amplify and harness the anti-tumor activity of the host immune system, reliable preclinical models that incorporate an intact immune response are desperately needed.

We characterized two new murine models of undifferentiated sarcoma maintained in a BALB/c background. Based on their doubling time, these tumors are highly aggressive. Both of these mouse sarcomas apparently arose from the subcutaneous implantation in immunocompromised C.B-17 SCID mice of surgical specimens of human brain tumor tissue from two different pediatric patients with medulloblastoma. Overgrowth of these two xenotumors with mouse tumors is an uncommon and largely unrecognized problem in establishing patient-derived xenografts in SCID mice. SCID mice seem to have a much higher propensity to develop sarcomas or lymphomas than athymic nudes, or Rag-1 or Rag-2 knockout mice, and most of the reports describe spontaneous mouse tumors in aged animals.[18,19] However, there are reports of mouse tumors arising after implantation of human cells.[18–21] Likely, the characteristically long initial tumor development time after implantation of human tumor tissue in immunocompromised mice could mask the local transformation of mouse muscle cells or thymic lymphocytes and subsequent overgrowth of the original implant. This possibility argues for the immediate testing of any nascent patient-derived xenograft with a prolonged development time to exclude its possible replacement and overgrowth of mouse tumor cells, which obviously occurred here with these two murine sarcomas.

Oncolytic viral therapy has seen recent advancement with US Food and Drug Administration (FDA) approval of talimogene laherparepvec (T-VEC) for the treatment of melanoma, and multiple clinical trials investigating oHSV therapy are under way.[22] A trial investigating a single intratumoral or intravenous injection of oHSV for patients with relapsed or refractory extracranial solid tumors including sarcomas is currently enrolling patients aged 7–30 years old (NCT00931931). Trials using oHSV with concurrent radiation (NCT02453191) or pembrolizumab, a programmed cell death protein-1 (PD-1) inhibitor (NCT03069378), are recruiting adults with advanced sarcoma.

Both SARC-28 and SARC-45 showed high cell surface expression of the primary HSV entry molecule CD111, suggesting that both sarcomas would be susceptible to infection by oHSV. We then confirmed these findings by conducting in vitro cytotoxicity and viral recovery assays, which showed that both sarcomas were sensitive to infection and killing by M002 at a relatively low concentration of M002. The in vitro HSV entry molecule expression and cytotoxicity data suggest that SARC-45 may be more susceptible than SARC-28 to infection with M002; however, the virus replicated equally in both cell lines after 24 hr of infection, and entry receptor molecule expression does not always correlate with higher viral entry.[23] Our in vivo studies examining the response to a single dose of M002 in immunocompromised mice bearing SARC-28 and SARC-45 in an immunoprivileged location confirmed the significant oncolytic effect of M002 in the absence of an adaptive host immune system. Previous studies demonstrated that human alveolar and embryonal rhabdomyosarcoma and renal sarcoma cell lines with high expression of CD111 were sensitive to in vitro killing by oHSV.[24,25] In vivo studies investigating oHSV for the treatment of human rhabdomyosarcoma xenografts and immunocompetent murine sarcomas demonstrated tumor shrinkage and protection from tumor re-challenge.[26,27] Waters et al.[28] demonstrated that multiple dosing of M002 reduced xenograft tumor growth and increased survival in mice bearing human alveolar and embryonal rhabdomyosarcoma.

Consistently, our in vivo flank studies demonstrated inhibition of tumor growth and extension of survival with a single dose of oHSV. Evaluation of the host immune response to treatment with M002 revealed a marked increase in tumor-infiltrating $CD4^+$ and $CD8^+$ T cells and $CD4^+$ and $CD8^+$ T cells with enhanced effector function, as indicated by intracellular interferon gamma (IFN-γ) and granzyme B expression compared to saline. Granzyme B, a serine protease that mediates cellular apoptosis in target cells, is upregulated by effector and memory $CD4^+$ and $CD8^+$ T cells upon activation and in the presence of IL-12.[29–31] In particular, compared to R3659 or saline treatment, tumors demonstrated increased activated monocytes after treatment with M002. Furthermore, the CD8:MDSC and CD8:Treg ratios were significantly higher at day 10 in M002 compared to R3659, suggesting that M002 creates a more favorable immune tumor microenvironment. Parker et al.[11] reported similar results in which M002 prolonged survival in intracranial glioma-bearing mice, and immunohistologic examination of tumor sections showed a significant influx of macrophages, $CD4^+$ cells, and $CD8^+$ cells in M002-treated tumors compared to R3659, as would be expected with the IL-12 expression that occurs during M002 replication and not with R3659 replication.

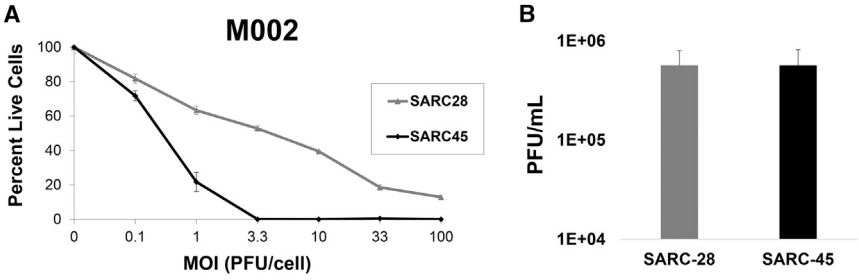

Figure 3. oHSV Cytotoxicity and Viral Recovery

(A) Sensitivity of SARC-28 and SARC-45 to M002 in vitro. The percentage of live cells was measured by the alamarBlue assay at a given MOI (plaque-forming units [PFU]/cell) compared to a control (no virus) after a 3-day incubation period. The average and SD of percent live cells were calculated from triplicate wells. (B) In vitro recovery rate of M002 in SARC-28 and SARC-45. Monolayers of tumor cells were infected with M002 at an MOI of 0.1 PFU/cell and at 24 hr post-infection, viral recovery was determined. The average and SD of PFU/mL were calculated from triplicate wells.

In contrast to the high sensitivity to killing by oHSV in vitro, the in vivo flank studies demonstrated a modest slowing in murine tumor growth and extension of survival in mice receiving a single dose of oHSV versus saline. There are a number of explanations for this: (1) cells in vitro are all at risk for virus infection, and the virus released from infected cells can easily spread to neighboring cells; (2) in vivo, the number of tumor cells that can be infected is much lower, and the ability of the released virus to percolate through complex tumor tissues is inhibited by stroma, extracellular matrix, and necrosis; and (3) given the rapid growth rate and short doubling time of both sarcomas, the therapeutic window may be more narrow because the tumor, which could be classified as bulky disease at the start of the virotherapy, outgrew the treatment effects of the virus. It takes about 40 hr before infectious HSV particles are released from infected cells, a critical issue since the doubling times of the tumors are comparably short. This is supported by the intracranial studies where fewer tumor cells were injected and the tumors were treated earlier resulting in a more effective anti-tumor result.

Another potential contributing factor to the differences in sensitivity seen in vitro compared to the in vivo flank studies is the immune response to the tumor and oHSV. Influx of immune cells has been demonstrated in all tumor types. Despite this apparent immune activation and localization, some tumors are able to evade and escape immune surveillance through various mechanisms. Among the immune cells infiltrating the tumor microenvironment are Tregs and MDSCs, immunosuppressive regulatory cells that contribute to the suppression of anti-tumor $CD4^+$ and $CD8^+$ T cells, leading to tumor immune escape.[32–36] Tumor-infiltrating and circulating MDSCs correlate with higher clinical cancer stage and extensive metastatic tumor burden in a variety of solid tumors.[37] In our studies, we found a significant increase in intratumoral Tregs after treatment with oHSV. This may suggest that oHSV therapy alone may not be sufficient to treat certain tumors that are prone to Treg infiltration or patients with large tumor burden. Consistent with this notion, although Cripe et al.[26] found virus-induced tumor infiltration by $CD4^+$ and $CD8^+$ T cells in a murine sarcoma model treated with oHSV, some sarcomas were resistant to virus-mediated killing. They attributed this finding to high levels of interleukin-10 (IL-10), an immunosuppressive cytokine produced by Tregs and MDSCs, suggesting that the presence of an immunosuppressive tumor microenvironment may have been limiting the function of anti-tumor $CD4^+$ and $CD8^+$ T cells.[26,34] Agents found to inhibit MDSCs and Tregs expand $CD4^+$ and $CD8^+$ T cells.[38–44]

In separate human xenograft sarcoma studies, depletion of MDSCs before and following oHSV injection resulted in enhanced tumor killing, and combination with alisertib, an aurora A kinase inhibitor, inhibited virus-provoked recruitment of intratumoral MDSCs in neuroblastoma and malignant peripheral nerve sheath tumor models.[45] Expansion of Tregs is associated with tumor expression of immunosuppressive checkpoint molecules such as cytotoxic T lymphocyte antigen-4 (CTLA-4), PD-1/programmed death-ligand 1 (PD-L1), and indolamine 2,3-dioxygenase (IDO).[46–48] Tregs themselves also express these proteins and are targetable via specific inhibitors.[49] Combination of oHSV with therapies that target Tregs, MDSCs, or checkpoint proteins is a potentially powerful synergistic regimen for treating solid tumors.

Novel therapies that act on the host immune system can only be reliably evaluated in models with intact immune response and function. SARC-28 and SARC-45 are newly described murine models of undifferentiated sarcoma maintained in an immunocompetent background and offer an exciting opportunity to further explore combination therapies that rely on an intact immune system to reach their full therapeutic potential.

MATERIALS AND METHODS

Murine Sarcoma Tumors and Genetically Engineered HSVs

SARC-28 and SARC-45 are murine sarcomas that arose spontaneously in immunocompromised SCID mice. Short tandem repeat analyses performed repeatedly on both cell lines by the Heflin Genomics Core (UAB) demonstrated the absence of any human DNA. SARC-28 and SARC-45 were maintained by serial transplantation in immunocompetent BALB/c mice. All animal studies were approved by the UAB Institutional Animal Care and Use Committee under the animal project number IACUC-08793 and conformed to all relevant regulatory standards.

Two genetically engineered, oncolytic herpes viruses, R3659 and M002, have been previously described.[11,50] R3659 is the parent virus for M002 with deletion of the native thymidine kinase locus and deleted regions of both $\gamma_1$34.5 loci. M002 is a conditionally replication-competent mutant human HSV that expresses both subunits

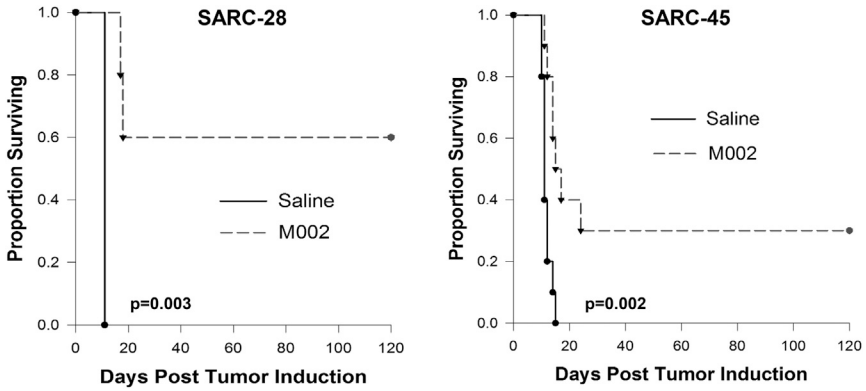

Figure 4. Kaplan-Meier Survival Plots

Athymic nude mice received an intracranial injection of 2–5 × 10^3 SARC-28 or SARC-45 cells. Three days after tumor implantation, mice received a single intratumoral injection of 10 μL of saline or 1 × 10^7 PFU of M002. Median survival was calculated. M002 significantly prolonged survival and resulted in several long-term survivors at 120 days.

of murine IL-12 (mIL-12). Transcription of *mIL-12* is under the control of the constitutively expressed murine early-growth response-1 promoter (Egr-1). M002 has previously been shown to produce IL-12 in physiologically relevant amounts in solid tumor models.

Tumor Disaggregation and Tissue Culture

Tumors were maintained by serial passage in BALB/c mice, aseptically harvested from the flanks of mice, and washed with PBS to remove excess blood and tissue debris. Tumors were minced with #11 scalpel blades, and minced tumors were disaggregated via gentleMACS Dissociator (Miltenyi Biotec, Auburn, CA, USA) per standard tumor protocol. Collected cells were washed twice with serumless DMEM/F12 (300 × *g*, 7 min, 4°C), counted in the presence of 0.04% trypan blue to enumerate viable cells and then used for study or added to NeuroBasal (NB) medium (Invitrogen, Grand Island, NY, USA) prepared with fibroblast growth factor-β (Invitrogen) and epidermal growth factor (Invitrogen) at 10 ng/mL, 2% B-27 supplement without vitamin A (Invitrogen), 2 mM L-glutamine, amphotericin B (250 μg/mL), and gentamicin (50 μg/mL). Vero cells were maintained using medium containing 7% fetal bovine serum. Medium was exchanged as needed, and cells grew adherently to the bottom of flasks. All cell cultures were maintained at 37°C, 20.8% O_2, and 5% CO_2.

Immunohistochemistry

Immunohistochemical examination of tissue sections was performed on 6-μm sections obtained from formalin-fixed, paraffin-embedded block preparations. The immunostaining for GFAP, CD45, and synaptophysin was accomplished with a semi-automated immunostainer (Dako Autostainer Link 48; Carpinteria, CA, USA) and an Envision FLEX HRP (horseradish peroxidase) system. Heat-induced epitope retrieval was accomplished with a 0.02 M concentration of citrate buffer (0.02 M [pH 9.0]) in a heater at 97°C for 20 min. The primary antibodies against GFAP (polyclonal rabbit; prediluted; Dako), synaptophysin (monoclonal mouse; clone SY38; prediluted; Dako), and CD45 (monoclonal mouse; clone UCHL-1; 1:1,000; Thermo Fisher Scientific Lab Vision, Waltham, MA, USA) were added. Fifteen-minute incubation with Envision FLEX Link (mouse or rabbit) was used as an enhancer. The chromogen diaminobenzidine tetrachloride (DAB) was used to visualize the antibody-antigen complex. The immunostaining for vimentin, S100 protein, CD99, and pan-cytokeratin was performed on a semi-automated immunostainer (Ventana, Tucson, AZ, USA) and an ultraView HPR Multimer approach. Heat-induced epitope retrieval with citrate buffer (0.02 M [pH 6.0]) CC1 in a heater at 120°C for 32 min was applied. The immunohistochemistry with prediluted antibodies from Ventana directed against vimentin (monoclonal mouse; clone 3B4), CD99 (monoclonal mouse; clone HO36-1.1), S100 protein (polyclonal rabbit), and pan-cytokeratin (AE1/AE3/PK26) incubated for 32 min. The chromogen diaminobenzidine tetrachloride was used to visualize the antibody-antigen complex. Finally, all the tissue sections were counterstained with hematoxylin. Appropriate positive and negative control slides were prepared. The negative control slides consisted of tissue sections of each case processed without the addition of primary antibody. All controls reacted appropriately.

Tumor Growth In Vivo

To characterize the growth rate of SARC-28 and SARC-45, we dissociated freshly harvested SARC-28 and SRAC-45 tumors into single-cell suspensions as above, then diluted them to achieve a 1 × 10^6 viable cells/50 μL suspension. BALB/c mice in groups of 10 were injected subcutaneously in the right flank with 1 × 10^6 cells, 3 × 10^6 cells, or 5 × 10^6 tumor cells in low growth factor Matrigel (Corning, Tewksbury, MA, USA). Tumors were measured twice weekly with calipers, and tumor volume in mm^3 was calculated using a standard formula [0.4($width^2$ × length)]. Once tumors reached a volume of 2,000 mm^3 or a length of 2 cm, mice were euthanized and tumors were harvested and processed for study.

Flow Cytometry

Expression levels of HSV entry molecules murine nectin-1 (CD111), nectin-2 (CD112), HVEM (CD270), and syndecan-2 were determined using two-color flow cytometry as we have previously described.[51] Tumors were harvested and dissociated into a single-cell suspension as described above. The following anti-mouse antibodies were used: CD111 (clone CK8; Invitrogen), CD112-phycoerythrin (PE) (clone 829038; R&D Systems, Minneapolis, MN, USA), CD270-PE (clone HMHV-1B18; BioLegend), and syndecan-2 polyclonal antibody (LifeSpan Biosciences, Seattle, WA, USA). PE-anti-mouse immunoglobulin G (IgG) Fc and allophycocyanin-anti-human IgG Fc (clone HP6017; BioLegend) were used as secondary antibodies for CD111 and SDC2, respectively. Samples were analyzed using a BD Biosciences (San Jose, CA, USA) FACSCalibur (UAB Flow Cytometry Core

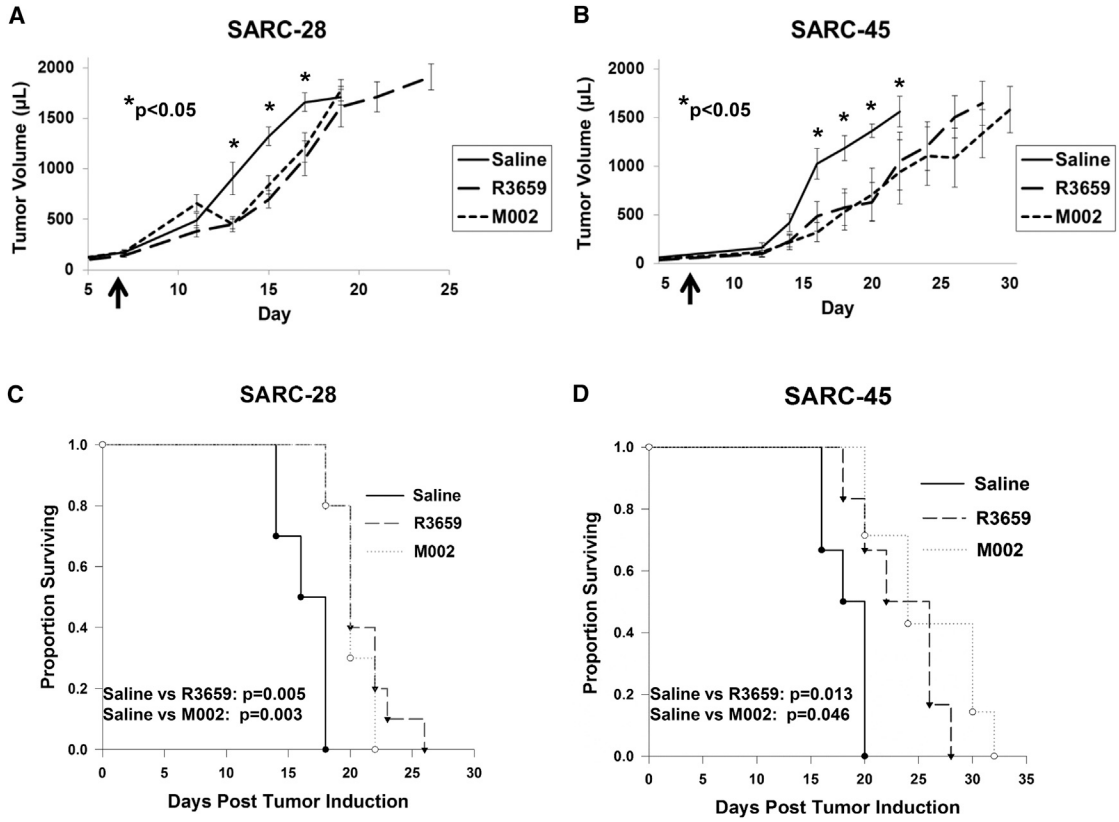

Figure 5. Mouse Survival and Tumor Growth versus oHSV

(A and B) Tumor growth curves of (A) SARC-28 and (B) SARC-45. Flank tumors in BALB/c mice received a single intratumoral injection of 20 μL of saline or 1×10^7 plaque-forming units (PFU) of R3659 or M002 (arrows). Tumor growth was measured twice weekly. Asterisks (*$p < 0.05$) indicate comparisons of saline to each oHSV treatment group (R3659 and M002) on that same experimental day. The average and SD of tumor volume (μL) were calculated from triplicate tumors. (C and D) Kaplan-Meier survival plots of (C) SARC-28 and (D) SARC-45 after treatment. Median survival time was calculated. M002 and R3659 significantly prolonged survival in both models.

Facility). Data were compiled using FlowJo (v10) software, and results are expressed as a percentage of gated cells.

In Vitro Cytotoxicity Assay

To assess the sensitivity of SARC-28 and SARC-45 cells to killing by oHSV in vitro, we measured cell viability 72 hr after virus treatment using an alamarBlue assay (Thermo Fisher Scientific). Cells were plated (1×10^5 viable cells/100 μL well) in 96-well plates, and after 24 hr were treated with 100 μL of saline or graded doses (0–100 PFU/cell) of M002. After 72 hr, 25 μL of alamarBlue was added to each well and incubated for 6–8 hr to detect metabolic activity as evidenced by reduction of the dye from dark blue to pink. Absorbance (optical density $[OD]_{595-562nm}$) was measured with a BioTek microplate spectrophotometer (Winooski, VT, USA), and the values were used to calculate numbers of PFU per cell required to kill 50% of the cells in a 3-day period, a lethal dose 50 (LD_{50}).

Viral Replication and Recovery

To assess the in vitro replication rate of M002 in SARC-28 and SARC-45, we grew cells to confluence in 6-well plates, infected them with 0.1 PFU/cell of M002, and incubated at 37°C. After 24 hr, cells were harvested by adding 1 mL of sterile milk and freezing at −80°C. Plates were thawed at 37°C, then underwent two more freeze/thaw cycles. Cells and supernatants were harvested, then sonicated for 15 s. Titers of progeny virions were determined using a 10-fold dilution series on confluent monolayers of Vero cells. The average and SD of PFU/mL were calculated from triplicate wells.

In Vivo Survival Study

Sensitivity of the sarcoma models to the viruses was determined in 6-week-old BALB/c mice. Mice were injected subcutaneously in the right flank with 1×10^6 SARC-28 or SARC-45 tumor cells in low growth factor Matrigel. Once tumors reached a volume of approximately 200 mm^3, mice were randomly divided into cohorts of 10 mice each and received one intratumoral injection of either normal saline (n = 10), R3659 (1×10^7 PFU/20 μL; n = 10), or M002 (1×10^7 PFU/20 μL; n = 10). Tumors were measured three times weekly with calipers, and tumor volume in mm^3 was calculated using a standard formula [$0.4(width^2 \times length)$]. Once tumors reached parameters dictated by institutional animal care and use

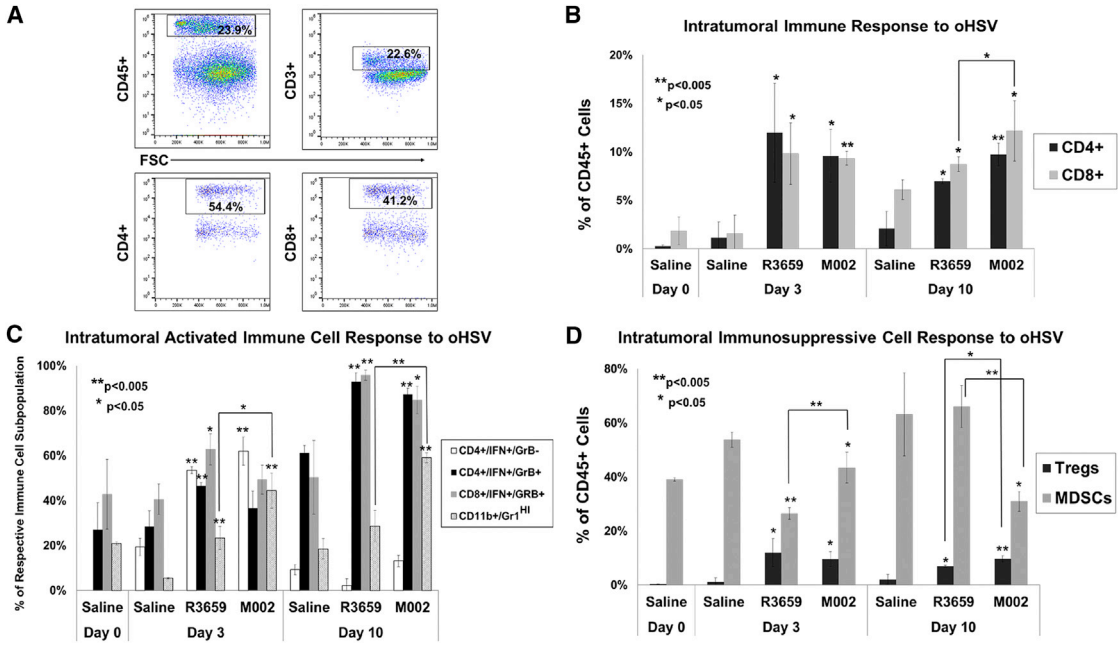

Figure 6. Intratumoral Immune Responses to Oncolytic HSV R3659 and M002 Compared to Saline

Flank tumors were injected with saline, R3659, or M002 and then harvested at days 3 and 10 and dissociated to single-cell suspension for flow cytometry. (A) Representative flow cytometry plots of $CD4^+$ and $CD8^+$ cells. (B) The frequencies of $CD4^+$ and $CD8^+$ T cells as a percentage of $CD45^+$ cells. (C) Activated monocytes ($CD11b^+/CDGr\text{-}1^{HI}$) as a percentage of all tumor-infiltrating immune cells ($CD45^+$), and activated $CD4^+$ or $CD8^+$ T cells with ($CD4^+/IFN^+/GrB^+$; $CD8^+/IFN^+/GrB^+$) and without ($CD4^+/IFN^+/GrB^-$) granzyme B expression as percentages of their respective lymphocyte subset. (D) Regulatory T cells (Tregs) and myeloid-derived suppressor cells (MDSCs; $CD11b^+/Gr\text{-}1^{INT}$) as a percentage of $CD45^+$ cells. Asterisks alone indicate comparisons of that group (R3659 or M002) to saline on that same experimental day. Asterisks over brackets indicate comparisons between oncolytic HSV (oHSV) treatment groups (R3659 versus M002) on the same experimental day. Significant differences between saline and each virus and between R3569 and M002 were determined by Student's t test. (B–D) The average and SD of cells were calculated from triplicate tumors.

committee (IACUC) protocol, mice were euthanized and tumors were harvested and processed for study.

To determine the oncolytic effect of the virus in an immunoprivileged model of sarcoma, nude mice were stereotactically injected intracerebrally with 2×10^5 SARC-28 or 5×10^5 SARC-45 cells. After 3 days, mice were randomly divided into cohorts of 10 mice each, and 1×10^7 PFU of M002 or saline vehicle was stereotactically inoculated at the same site of tumor injection. Mice were assessed daily, moribund mice were euthanized, and the date of death was recorded.

Immune Response Study

In order to characterize the intratumoral immune response to treatment with oHSV, we implanted 6-week-old BALB/c immunocompetent mice subcutaneously with 1×10^6 SARC-28 tumor cells in low growth factor Matrigel into the right flank. Once tumors reached a volume of approximately 200 mm^3, mice were randomly divided into cohorts of 10 mice each and received one intratumoral injection of either normal saline (n = 10), R3659 (1×10^7 PFU/20 μL; n = 10), or M002 (1×10^7 PFU/20 μL; n = 10). Day of virus injection was deemed "day 0." On day 0, three mice from the saline group were sacrificed, and tumors were processed for study. On days 3 and 10, three mice from each treatment group were sacrificed, and tumors were processed for study.

On each harvest day, tumors were individually dissociated into single-cell suspensions, and each was stained for the presence of surface and intracellular proteins. The first antibody panel included surface staining for the leukocyte marker CD45-allophycocyanin, T cell marker CD3-PercPcy5.5, T helper cell marker CD4-BV510, T cytotoxic cell marker CD8-BV605, and Treg marker CD25-allophycocyanin.cy7, followed by intracellular staining for the Treg transcription factor FOXP3-PE.cy7. The second antibody panel included surface staining for CD45-allophycocyanin, B cell marker CD19-PerPcy5.5, macrophage and monocyte marker CD11b-FITC, granulocyte and monocyte marker Gr-1(Ly-6G/Ly-6C)-Pacific Blue, and monocyte marker Ly6C-Pe.cy7. To assess the ability of intratumoral T lymphocytes to become activated and mount an immune response, we added Leukocyte Activation Cocktail, with BD GolgiPlug (BD Biosciences), to a 1×10^6 tumor cell suspension and incubated it at 37°C for 5 hr. Samples were then analyzed using the third panel of antibodies, which included surface staining for CD45-allophycocyanin, CD3-PercPcy5.5, CD4-BV510, and CD8-BV605, followed by intracellular staining for markers indicating T cell effector activity, granzyme B-Pacific Blue, and interferon gamma (IFN-γ)-PE.cy7. For

intracellular staining, cells were fixed and permeabilized using the True-Nuclear transcription factor fixation/permeabilization buffer set (BioLegend). Samples were then acquired using a Thermo Fisher Attune Nxt Flow Cytometer (UAB Flow Cytometry Core Facility). Data were analyzed using FlowJo software V10 (Tristar).

Statistical Analysis

All experiments were done in triplicate. Student's t test analyses for significance of mean differences were performed using Microsoft Excel (Microsoft, Redmond, WA, USA). $p \leq 0.05$ was considered significant. SigmaPlot version 12.0 (Systat Software, San Jose, CA, USA) was used to generate survival curves using Kaplan-Meier analysis and median survival time. To compare groups, we applied the log rank test.

AUTHOR CONTRIBUTIONS

Study Conception and Design: E.K.R., J.W.L., G.Y.G., G.K.F.; Acquisition of Data: E.K.R., B.P.M., L.N., V.M.K.; Analysis and Interpretation of Data: E.K.R., R.L., X.H., E.A.B., J.M.M., J.W.L., G.Y.G., G.K.F.; Writing – Drafting of Manuscript: E.K.R., G.K.F.; Writing – Critical Revision: E.K.R., R.L., X.H., E.A.B., J.M.M., J.W.L., G.Y.G., G.K.F.

CONFLICTS OF INTEREST

G.Y.G. is a founder of and owns stock and stock options (<10%) in Maji Therapeutics, which is developing other HSVs that are not the subject of the current investigation. J.M.M. and G.Y.G. were also founders of and owned stock and stock options (<8%) in Catherex Inc., a biotechnology company that had licensed additional intellectual property related to oHSV. Catherex, Inc. was sold to Amgen, Inc. in a structured buyout on December 18, 2015, and they no longer participate in any decision making or have any control of any aspect of Catherex or Amgen, although they did receive proceeds from the sale of the company. They also are founders and hold stock in another OV-related company, Aettis, Inc. G.Y.G. has served as a paid advisor to the Program Project at the Ohio State University that seeks to find improved methods for application of distinct oHSV to treat localized and metastatic cancers. This is generally, but not specifically, related to the subject matter of this investigation.

ACKNOWLEDGMENTS

This work was supported in part by grants from St. Baldrick's Foundation (to G.F.K.), the Rally Foundation for Childhood Cancer Research (to G.F.K.), the Truth 365, Hyundai Hope on Wheels (to G.K.F.), and the NIH (grants P01CA071933 and P50CA151129 to J.M.M. and G.Y.G.). We thank the Analytic and Preparative Core Facility (supported by NIH grants P30 AR048311 and P30 AI27667) for assistance with flow cytometry and Michael Crowley, PhD, and the Heflin Center for Genomic Science (supported by grant CA13148-40) for assistance with short tandem repeat (STR) profiling.

REFERENCES

1. Ng, V.Y., Scharschmidt, T.J., Mayerson, J.L., and Fisher, J.L. (2013). Incidence and survival in sarcoma in the United States: a focus on musculoskeletal lesions. Anticancer Res. *33*, 2597–2604.
2. Kaatsch, P. (2010). Epidemiology of childhood cancer. Cancer Treat. Rev. *36*, 277–285.
3. van der Graaf, W.T., Orbach, D., Judson, I.R., and Ferrari, A. (2017). Soft tissue sarcomas in adolescents and young adults: a comparison with their paediatric and adult counterparts. Lancet Oncol. *18*, e166–e175.
4. Fidler, M.M., Frobisher, C., Guha, J., Wong, K., Kelly, J., Winter, D.L., Sugden, E., Duncan, R., Whelan, J., Reulen, R.C., and Hawkins, M.M. (2015). Long-term adverse outcomes in survivors of childhood bone sarcoma: the British Childhood Cancer Survivor Study. Br. J. Cancer *112*, 1857–1865.
5. Ferrari, A., Sultan, I., Huang, T.T., Rodriguez-Galindo, C., Shehadeh, A., Meazza, C., Ness, K.K., Casanova, M., and Spunt, S.L. (2011). Soft tissue sarcoma across the age spectrum: a population-based study from the Surveillance Epidemiology and End Results database. Pediatr. Blood Cancer *57*, 943–949.
6. Spunt, S.L., Poquette, C.A., Hurt, Y.S., Cain, A.M., Rao, B.N., Merchant, T.E., Jenkins, J.J., Santana, V.M., Pratt, C.B., and Pappo, A.S. (1999). Prognostic factors for children and adolescents with surgically resected nonrhabdomyosarcoma soft tissue sarcoma: an analysis of 121 patients treated at St Jude Children's Research Hospital. J. Clin. Oncol. *17*, 3697–3705.
7. Stahl, M., Ranft, A., Paulussen, M., Bölling, T., Vieth, V., Bielack, S., Görtitz, I., Braun-Munzinger, G., Hardes, J., Jürgens, H., and Dirksen, U. (2011). Risk of recurrence and survival after relapse in patients with Ewing sarcoma. Pediatr. Blood Cancer *57*, 549–553.
8. Rodriguez-Galindo, C., Shah, N., McCarville, M.B., Billups, C.A., Neel, M.N., Rao, B.N., and Daw, N.C. (2004). Outcome after local recurrence of osteosarcoma: the St. Jude Children's Research Hospital experience (1970-2000). Cancer *100*, 1928–1935.
9. Pappo, A.S., Devidas, M., Jenkins, J., Rao, B., Marcus, R., Thomas, P., Gebhardt, M., Pratt, C., and Grier, H.E. (2005). Phase II trial of neoadjuvant vincristine, ifosfamide, and doxorubicin with granulocyte colony-stimulating factor support in children and adolescents with advanced-stage nonrhabdomyosarcomatous soft tissue sarcomas: a Pediatric Oncology Group Study. J. Clin. Oncol. *23*, 4031–4038.
10. Chou, J., Kern, E.R., Whitley, R.J., and Roizman, B. (1990). Mapping of herpes simplex virus-1 neurovirulence to gamma 134.5, a gene nonessential for growth in culture. Science *250*, 1262–1266.
11. Parker, J.N., Gillespie, G.Y., Love, C.E., Randall, S., Whitley, R.J., and Markert, J.M. (2000). Engineered herpes simplex virus expressing IL-12 in the treatment of experimental murine brain tumors. Proc. Natl. Acad. Sci. USA *97*, 2208–2213.
12. Kishima, H., Shimizu, K., Miyao, Y., Mabuchi, E., Tamura, K., Tamura, M., Sasaki, M., and Hakakawa, T. (1998). Systemic interleukin 12 displays anti-tumour activity in the mouse central nervous system. Br. J. Cancer *78*, 446–453.
13. Meko, J.B., Tsung, K., and Norton, J.A. (1996). Cytokine production and antitumor effect of a nonreplicating, noncytopathic recombinant vaccinia virus expressing interleukin-12. Surgery *120*, 274–282, discussion 282–283.
14. Markert, J.M., Cody, J.J., Parker, J.N., Coleman, J.M., Price, K.H., Kern, E.R., Quenelle, D.C., Lakeman, A.D., Schoeb, T.R., Palmer, C.A., et al. (2012). Preclinical evaluation of a genetically engineered herpes simplex virus expressing interleukin-12. J. Virol. *86*, 5304–5313.
15. Patel, D.M., Foreman, P.M., Nabors, L.B., Riley, K.O., Gillespie, G.Y., and Markert, J.M. (2016). Design of a phase I clinical trial to evaluate M032, a genetically engineered HSV-1 expressing IL-12, in patients with recurrent/progressive glioblastoma multiforme, anaplastic astrocytoma, or gliosarcoma. Hum. Gene Ther. Clin. Dev. *27*, 69–78.
16. Houghton, P.J., Morton, C.L., Tucker, C., Payne, D., Favours, E., Cole, C., Gorlick, R., Kolb, E.A., Zhang, W., Lock, R., et al. (2007). The pediatric preclinical testing program: description of models and early testing results. Pediatr. Blood Cancer *49*, 928–940.
17. Krummenacher, C., Baribaud, F., Ponce de Leon, M., Baribaud, I., Whitbeck, J.C., Xu, R., Cohen, G.H., and Eisenberg, R.J. (2004). Comparative usage of herpesvirus entry mediator A and nectin-1 by laboratory strains and clinical isolates of herpes simplex virus. Virology *322*, 286–299.
18. Huang, P., Westmoreland, S.V., Jain, R.K., and Fukumura, D. (2011). Spontaneous nonthymic tumors in SCID mice. Comp. Med. *61*, 227–234.

19. Santagostino, S.F., Arbona, R.J.R., Nashat, M.A., White, J.R., and Monette, S. (2017). Pathology of aging in NOD scid gamma female mice. Vet. Pathol. *54*, 855–869.

20. Kavirayani, A.M., and Foreman, O. (2010). Retrospective study of spontaneous osteosarcomas in the nonobese diabetic strain and nonobese diabetic-derived substrains of mice. Vet. Pathol. *47*, 482–487.

21. Bosma, M.J., and Carroll, A.M. (1991). The SCID mouse mutant: definition, characterization, and potential uses. Annu. Rev. Immunol. *9*, 323–350.

22. Bommareddy, P.K., Patel, A., Hossain, S., and Kaufman, H.L. (2017). Talimogene laherparepvec (T-VEC) and other oncolytic viruses for the treatment of melanoma. Am. J. Clin. Dermatol. *18*, 1–15.

23. Wang, P.Y., Swain, H.M., Kunkler, A.L., Chen, C.Y., Hutzen, B.J., Arnold, M.A., Streby, K.A., Collins, M.H., Dipasquale, B., Stanek, J.R., et al. (2016). Neuroblastomas vary widely in their sensitivities to herpes simplex virotherapy unrelated to virus receptors and susceptibility. Gene Ther. *23*, 135–143.

24. Pressey, J.G., Haas, M.C., Pressey, C.S., Kelly, V.M., Parker, J.N., Gillespie, G.Y., and Friedman, G.K. (2013). CD133 marks a myogenically primitive subpopulation in rhabdomyosarcoma cell lines that are relatively chemoresistant but sensitive to mutant HSV. Pediatr. Blood Cancer *60*, 45–52.

25. Megison, M.L., Gillory, L.A., Stewart, J.E., Nabers, H.C., Mroczek-Musulman, E., Waters, A.M., Coleman, J.M., Kelly, V., Markert, J.M., Gillespie, G.Y., et al. (2014). Preclinical evaluation of engineered oncolytic herpes simplex virus for the treatment of pediatric solid tumors. PLoS ONE *9*, e86843.

26. Leddon, J.L., Chen, C.Y., Currier, M.A., Wang, P.Y., Jung, F.A., Denton, N.L., Cripe, K.M., Haworth, K.B., Arnold, M.A., Gross, A.C., et al. (2015). Oncolytic HSV virotherapy in murine sarcomas differentially triggers an antitumor T-cell response in the absence of virus permissivity. Mol. Ther. Oncolytics *1*, 14010.

27. Currier, M.A., Adams, L.C., Mahller, Y.Y., and Cripe, T.P. (2005). Widespread intratumoral virus distribution with fractionated injection enables local control of large human rhabdomyosarcoma xenografts by oncolytic herpes simplex viruses. Cancer Gene Ther. *12*, 407–416.

28. Waters, A.M., Stafman, L.L., Garner, E.F., Mruthyunjayappa, S., Stewart, J.E., Friedman, G.K., Coleman, J.M., Markert, J.M., Gillespie, G.Y., and Beierle, E.A. (2016). Effect of repeat dosing of engineered oncolytic herpes simplex virus on preclinical models of rhabdomyosarcoma. Transl. Oncol. *9*, 419–430.

29. Bossi, G., Trambas, C., Booth, S., Clark, R., Stinchcombe, J., and Griffiths, G.M. (2002). The secretory synapse: the secrets of a serial killer. Immunol. Rev. *189*, 152–160.

30. Lin, L., Couturier, J., Yu, X., Medina, M.A., Kozinetz, C.A., and Lewis, D.E. (2014). Granzyme B secretion by human memory CD4 T cells is less strictly regulated compared to memory CD8 T cells. BMC Immunol. *15*, 36.

31. Rubinstein, M.P., Su, E.W., Suriano, S., Cloud, C.A., Andrijauskaite, K., Kesarwani, P., Schwartz, K.M., Williams, K.M., Johnson, C.B., Li, M., et al. (2015). Interleukin-12 enhances the function and anti-tumor activity in murine and human CD8(+) T cells. Cancer Immunol. Immunother. *64*, 539–549.

32. Williams, L.M., and Rudensky, A.Y. (2007). Maintenance of the Foxp3-dependent developmental program in mature regulatory T cells requires continued expression of Foxp3. Nat. Immunol. *8*, 277–284.

33. Fiorentino, D.F., Zlotnik, A., Vieira, P., Mosmann, T.R., Howard, M., Moore, K.W., and O'Garra, A. (1991). IL-10 acts on the antigen-presenting cell to inhibit cytokine production by Th1 cells. J. Immunol. *146*, 3444–3451.

34. Chaudhry, A., Samstein, R.M., Treuting, P., Liang, Y., Pils, M.C., Heinrich, J.M., Jack, R.S., Wunderlich, F.T., Brüning, J.C., Müller, W., and Rudensky, A.Y. (2011). Interleukin-10 signaling in regulatory T cells is required for suppression of Th17 cell-mediated inflammation. Immunity *34*, 566–578.

35. Wang, K., and Vella, A.T. (2016). Regulatory T cells and cancer: a two-sided story. Immunol. Invest. *45*, 797–812.

36. Kusmartsev, S., and Gabrilovich, D.I. (2002). Immature myeloid cells and cancer-associated immune suppression. Cancer Immunol. Immunother. *51*, 293–298.

37. Diaz-Montero, C.M., Salem, M.L., Nishimura, M.I., Garrett-Mayer, E., Cole, D.J., and Montero, A.J. (2009). Increased circulating myeloid-derived suppressor cells correlate with clinical cancer stage, metastatic tumor burden, and doxorubicin-cyclophosphamide chemotherapy. Cancer Immunol. Immunother. *58*, 49–59.

38. Le, H.K., Graham, L., Cha, E., Morales, J.K., Manjili, M.H., and Bear, H.D. (2009). Gemcitabine directly inhibits myeloid derived suppressor cells in BALB/c mice bearing 4T1 mammary carcinoma and augments expansion of T cells from tumor-bearing mice. Int. Immunopharmacol. *9*, 900–909.

39. Vincent, J., Mignot, G., Chalmin, F., Ladoire, S., Bruchard, M., Chevriaux, A., Martin, F., Apetoh, L., Rébé, C., and Ghiringhelli, F. (2010). 5-Fluorouracil selectively kills tumor-associated myeloid-derived suppressor cells resulting in enhanced T cell-dependent antitumor immunity. Cancer Res. *70*, 3052–3061.

40. Kodumudi, K.N., Weber, A., Sarnaik, A.A., and Pilon-Thomas, S. (2012). Blockade of myeloid-derived suppressor cells after induction of lymphopenia improves adoptive T cell therapy in a murine model of melanoma. J. Immunol. *189*, 5147–5154.

41. Mirza, N., Fishman, M., Fricke, I., Dunn, M., Neuger, A.M., Frost, T.J., Lush, R.M., Antonia, S., and Gabrilovich, D.I. (2006). All-trans-retinoic acid improves differentiation of myeloid cells and immune response in cancer patients. Cancer Res. *66*, 9299–9307.

42. Veltman, J.D., Lambers, M.E., van Nimwegen, M., Hendriks, R.W., Hoogsteden, H.C., Aerts, J.G., and Hegmans, J.P. (2010). COX-2 inhibition improves immunotherapy and is associated with decreased numbers of myeloid-derived suppressor cells in mesothelioma. Celecoxib influences MDSC function. BMC Cancer *10*, 464.

43. Veltman, J.D., Lambers, M.E., van Nimwegen, M., Hendriks, R.W., Hoogsteden, H.C., Hegmans, J.P., and Aerts, J.G. (2010). Zoledronic acid impairs myeloid differentiation to tumour-associated macrophages in mesothelioma. Br. J. Cancer *103*, 629–641.

44. Melani, C., Sangaletti, S., Barazzetta, F.M., Werb, Z., and Colombo, M.P. (2007). Amino-biphosphonate-mediated MMP-9 inhibition breaks the tumor-bone marrow axis responsible for myeloid-derived suppressor cell expansion and macrophage infiltration in tumor stroma. Cancer Res. *67*, 11438–11446.

45. Currier, M.A., Sprague, L., Rizvi, T.A., Nartker, B., Chen, C.Y., Wang, P.Y., Hutzen, B.J., Franczek, M.R., Patel, A.V., Chaney, K.E., et al. (2017). Aurora A kinase inhibition enhances oncolytic herpes virotherapy through cytotoxic synergy and innate cellular immune modulation. Oncotarget *8*, 17412–17427.

46. Peggs, K.S., Quezada, S.A., Chambers, C.A., Korman, A.J., and Allison, J.P. (2009). Blockade of CTLA-4 on both effector and regulatory T cell compartments contributes to the antitumor activity of anti-CTLA-4 antibodies. J. Exp. Med. *206*, 1717–1725.

47. Highfill, S.L., Cui, Y., Giles, A.J., Smith, J.P., Zhang, H., Morse, E., Kaplan, R.N., and Mackall, C.L. (2014). Disruption of CXCR2-mediated MDSC tumor trafficking enhances anti-PD1 efficacy. Sci. Transl. Med. *6*, 237ra67.

48. Holmgaard, R.B., Zamarin, D., Li, Y., Gasmi, B., Munn, D.H., Allison, J.P., Merghoub, T., and Wolchok, J.D. (2015). Tumor-expressed IDO recruits and activates MDSCs in a Treg-dependent manner. Cell Rep. *13*, 412–424.

49. Ring, E.K., Markert, J.M., Gillespie, G.Y., and Friedman, G.K. (2017). Checkpoint proteins in pediatric brain and extracranial solid tumors: opportunities for immunotherapy. Clin. Cancer Res. *23*, 342–350.

50. Gillory, L.A., Megison, M.L., Stewart, J.E., Mroczek-Musulman, E., Nabers, H.C., Waters, A.M., Kelly, V., Coleman, J.M., Markert, J.M., Gillespie, G.Y., et al. (2013). Preclinical evaluation of engineered oncolytic herpes simplex virus for the treatment of neuroblastoma. PLoS ONE *8*, e77753.

51. Friedman, G.K., Langford, C.P., Coleman, J.M., Cassady, K.A., Parker, J.N., Markert, J.M., and Yancey Gillespie, G. (2009). Engineered herpes simplex viruses efficiently infect and kill CD133+ human glioma xenograft cells that express CD111. J. Neurooncol. *95*, 199–209.